Poly(ethylene oxide)–Sodium Polyiodide Conductors: Characterization, Electrical Conductivity, and Photoresponse

L. Charles Hardy and Duward F. Shriver*

Contribution from the Department of Chemistry, Northwestern University, Evanston, Illinois 60201. *Received November 1, 1985*

Abstract: The complexes of poly(ethylene oxide) with sodium polyiodide are electronic conductors. The level of conductivity at room temperature is 2 to 3 orders of magnitude greater than that of simple quaternary ammonium polyiodide salts. Raman spectroscopy indicates that the polyiodide species formed in the polymeric material depends upon the salt concentration in the polymer as well as the iodine to sodium ion ratio. High conductivity is associated with the appearance of a polyiodide species having a resonance-enhanced Raman feature at ca. 171 cm^{-1}. A photovoltaic effect is observed when the polyiodide-containing polymer is sandwiched between indium–tin oxide glass and platinum electrodes and then illuminated through the ITO. The sign of the photoinduced potential indicates that the photovoltaic effect arises from a recombination of electrons from ITO with holes in the polyiodide valance bond.

Electrically conducting polymers and redox polymers have attracted considerable attention in recent years. Among these materials are solvent-free polymeric electronic conductors,[1,2] solvent-free ionic conductors,[3] and solvent-swollen redox polymers.[4] These conducting polymers are of interest from the standpoints of synthesis of new materials, the origin of their charge transport mechanisms, and their potential applications in electrochemical devices. For example, solid electrolytes have been investigated for use in high energy density batteries,[5] solid-state photoelectrochemical cells,[6,7] and electrochemistry in ultra-high vacuum.[8] Most studies of polymer electrolytes have focused on the factors influencing ion transport, with an emphasis on achieving high cation transport and negligible electronic conductivity or redox activity. The majority of solvent-free polymer electrolytes have been prepared by complex formation between a polyether and a simple alkali metal salt.

In the present research we have utilized a polyether, poly(ethylene oxide), as a host for alkali metal polyiodides. The polyiodides are potentially electrical conductors through ionic and electronic (or hole) charge transport. They also should display redox and photochemical activity. In the latter connection, we have investigated a polyiodide-containing polymer in a photovoltaic cell.

Experimental Section

Poly(ethylene oxide), MW 600000 (Aldrich), and reagent grade solvents, NaI and I_2, were normally used as received. Chemicals were also used after drying and purification as described elsewhere.[9] Standard inert atmosphere techniques were employed for preparation and characterization of samples unless otherwise stated. Polymer electrolytes were formed by dissolving preweighed amounts of polymer and salt in acetonitrile followed by dropwise addition of the desired stoichiometric amount of I_2 in acetonitrile to the stirring polymer solution. A typical preparation was on a 0.6-g scale with about 15 mL of acetonitrile. After a homogeneous solution was obtained, solvent was removed under vacuum to give a polymer film. Drying the film under vacuum (0.01 torr) for 12 h resulted in loss of only a few milligrams of I_2 from the sample; the solvent which was condensed at −196 °C and then thawed was only very slightly colored by I_2. IR spectroscopy indicated absence of residual solvent or water to the limits of detection which were determined to be 2 ppt and 100 ppm, respectively, using a method previously described.[10] Elemental analyses were performed by Galbraith Laboratories, Inc.: Anal. Calcd for $[(CH_2CH_2O)_4NaI_3]_n$: C, 16.56; H, 2.78; Na, 3.97; I, 65.66. Found: C, 16.06; H, 2.94; Na, 3.79; I, 65.59. Calcd for $[(CH_2CH_2O)_4NaI_2]_n$: C, 21.20; H, 3.56; Na, 5.08; I, 56.04. Found: C, 20.79; H, 3.94; Na, 4.69; I, 55.47.

Proton and carbon NMR spectra were obtained on a JEOL FX 90Q (^1H 89.55 MHz; ^{13}C 22.49 MHz); samples were dissolved in CD_3CN and chemical shifts were referenced to external Me_4Si. Diffuse reflectance electronic and near-IR spectra were recorded on a Cary Model 17D spectrophotometer with a Model 1411 diffuse reflectance attachment. Transmission electronic spectra were recorded on a Perkin-Elmer 330 spectrophotometer. Electronic spectra were normally run with samples exposed to air; samples sealed from air gave essentially the same results. Laser Raman spectra were recorded with Kr^+ (413.1, 568.2, 676.4 nm) or Ar^+ (457.9, 476.5, 488.0, 496.5, 514.6 nm) excitation and a Spex 1401 monochromator with photon counting detection. Spectral resolution was normally 3 cm^{-1}. Solid samples were sealed under an inert atmosphere in 5-mm Pyrex tubes. All samples were probed with a 180° backscattering geometry,[11] and spinning was employed to reduce localized heating in the samples. Spectra were calibrated with the exciting line. For polarization studies, fibers were oriented by stretching thin, narrow films (not completely dry) cast from acetonitrile onto glass plates. Elongation, on the order of 300–400%, was maintained by attaching the fibers to a rigid backing and then drying as previously described. Fibers were placed in 5-mm tubes with the fibers parallel to the spinning axis.

Differential scanning calorimetry (DSC) was performed as previously described.[10,12] Samples were loaded under an argon atmosphere in hermetically sealed aluminum pans. Because of the possible reaction of polyiodide species with aluminum, some samples were placed between two pieces of Teflon tape before the pans were sealed. This procedure provided separation of the sample from the sample pan. Results for samples in the two different types of sample holders were virtually the same except for the appearance of endotherms for Teflon tape, which did not occur in the same temperature regions as sample transitions. As an additional check, sample pans were opened and examined after the experiments. Neither corrosion of aluminum nor coloration

(1) *Polymers in Electronics*; Davidson, T., Ed.; American Chemical Society: Washington, DC. 1984.
(2) Marks, T. J. *Science (Washington, DC)* **1985**, *277*, 881–889.
(3) Armand, M. *Solid State Ionics* **1983**, *9* and *10*, 745–754.
(4) Murray, R. W. *Annu. Rev. Mater. Sci.* **1984**, *14*, 145–169.
(5) Gauthier, M.; Fauteux, D.; Vassort, G.; Belanger, A.; Duval, M.; Ricoux, P.; Chabagno, J.-M.; Muller, D.; Rigaud, P.; Armand, M. B.; Deroo, D. *J. Electrochem. Soc.* **1985**, *132*, 1333–1340.
(6) Skotheim, T.; Lundstrom, I. *J. Electrochem. Soc.* **1982**, *129*, 894–896.
(7) Sammells, A. F.; Ang, P. G. P. *J. Electrochem. Soc.* **1984**, *131*, 617–619.
(8) Skotheim, T. A.; Florit, M. I.; Melo, A.; O'Grady, W. E. *Phys. Rev. B: Condens. Matter* **1984**, *30*, 4846–4849.
(9) Papke, B. L.; Ratner, M. A.; Shriver, D. F. *J. Phys. Chem. Solids* **1981**, *42*, 493–500.
(10) Hardy, L. C.; Shriver, D. F. *J. Am. Chem. Soc.* **1985**, *107*, 3823–3828.
(11) Shriver, D. F.; Dunn, J. B. R. *J. Appl. Spectrosc.* **1974**, *88*, 319–323.

0002-7863/86/1508-2887$01.50/0

Table I. Constitution, Color, and Raman Data for PEO–Sodium Polyiodide Complexes

compd	mol ratio $-CH_2CH_2O-$	NaI	I_2	color	Raman freq, cm^{-1}	
1	3	1	1/4	brown-red		116
2	3	1	1/2	red-black	171	116
3	4	1	1/2	brown-red		116
4	4	1	1	blue-black	175, 167	
5	8	1	1	red-black	171	113

of Teflon tape by iodine was apparent. X-ray diffraction data were obtained as previously described.[12]

AC impedance measurements over the frequency range 5 to 5×10^5 Hz were performed as previously described;[10,12] samples were placed between Pt disk electrodes, under an inert atmosphere, in a sealed sample holder. Current–voltage response was measured with a PAR Model 363 potentiostat–galvanostat, a potentiostat controller built in-house, and an XY recorder.

Photoresponse measurements were made with the xenon light source and monochromator of a Hitachi Perkin-Elmer MPF-2A fluorescence spectrophotometer. A 16-nm band-pass was used, and light intensities at the various wavelengths were normalized by using intensity measurements performed with a Model 40X opto-meter from United Detector Technology. Intensities were normalized to a value of approximately 0.6 mW/cm^2. Open circuit voltages and short-circuit currents were measured with a Keithley Model 177 microvolt digital multimeter Tin-doped indium oxide (ITO) coated glass (80 ohm/square or 5 ohm/square) was obtained from Donnelly Mirrors, Inc. Photoresponse measurements were made on films (50–200 μm) sandwiched between ITO glass and platinum electrodes and illuminated through the ITO glass electrode; samples were briefly exposed to air during cell fabrication. Better contacts and, therefore, better current densities were obtained if the films, sandwiched between electrodes with slight pressure, were heated to about 60 °C (under inert atmospheric conditions) where slight flow of the polymer occurred. Thermoelectric power measurements were made by placing two point probes (Pt) of different temperatures (25 and ~60 or 25 °C and a probe dipped in liquid N_2) on a sample film (in air).

Results and Discussion

Salts of a wide variety of anions may be incorporated into poly(ethylene oxide) (PEO). The conductivities of these materials, as well as other evidence,[9,13] indicate that the anion and cation are separated by the polymer. This separation appears desirable for the stabilization of polyiodide anions because the polyiodide salts are known only in conjunction with large cations.[14,15] For example, NaI_3 and higher sodium polyiodides are unknown, but a wide variety of tetraalkylammonium polyiodides are known. As described in the introduction, it is indeed possible to prepare sodium polyiodides in PEO (eq 1). The composition of these polymer–salt complexes is designated as follows: $(PEO)_xNaI_{1+2y}$, where PEO represents the polymer repeat unit $(-C_2H_4O)-$ and y represents the molar ratio of I_2 to NaI. The resulting polymer

$$NaI(s) + xPEO(s) \xrightarrow{CH_3CN} PEO_xNaI(solution) \xrightarrow{yI_2 \text{ in } CH_3CN} PEO_xNaI_{1+2y}(solution) \xrightarrow{-CH_3CH} PEO_xNaI_{1+2y}(s) \quad (1)$$

complexes were dark, semicrystalline films which were characterized by chemical, thermal, and spectroscopic methods, X-ray diffraction, and electrical measurements.

Chemical and Physical Characterization of Polymer–Salt Complexes. The composition and appearance of the compounds studied are listed in Table I. The most striking difference among the materials formed is the brown-red color of $PEO_3NaI_{1.5}$ (**1**) and PEO_4NaI_2 (**3**) in comparison to blue-black PEO_4NaI_3 (**4**). These colors are typical of crystalline, polyiodide salts.[15] Samples of **1** and **3** are stable against loss of I_2 up to at least a year. By contrast, when PEO_3NaI_2 (**2**), $(PEO)_4NaI_3$ **4**, and PEO_8NaI_3 (**5**) are left open to the atmosphere I_2 is lost; this is typical of many polyhalide salts.[15]

The possibility of a reaction between iodine and the polymer backbone was investigated by ^1H and ^{13}C NMR spectroscopy. PEO–sodium polyiodide complexes are soluble in acetone or acetonitrile, indicating that no cross-linking has occurred. NMR data collected on samples of PEO_4NaI, PEO_4NaI plus I_2, dissolved in CD_3CN have a singlet in their proton NMR spectra and a singlet in their decoupled ^{13}C spectra. Only slight shifts from the resonances for PEO are observed owing to the presence of added salt; significantly, no additional peaks are found which might arise from halogenation of the polymer backbone. These PEO complexes contrast with the poly(2-vinylpyridine)–iodine (P2VP–I_2) systems which are used as cathodes in lithium batteries and are normally produced by reaction at elevated temperatures (125–150 °C) for a few days. These cathode materials are cross-linked complex mixtures for which reaction between I_2 and the polymer has been reported.[16]

In agreement with published differential scanning calorimetric data for simple PEO–NaI complexes,[17-20] the 3:1 and 4:1 PEO·NaI complexes[17-20] exhibit endothermic peaks at ca. 463 and ca. 338 K. The higher temperature peak is attributed to melting of the salt-rich polymer complex in both electrolytes whereas the lower melting peak is attributed to melting of a pure PEO phase in the 4:1 electrolyte. The low-temperature transition is of uncertain origin in the 3:1 electrolyte. For the PEO_4NaI_2 complex (**3**), however, only a single endothermic melt is seen at 410 K; no peaks are seen for the melting of pure PEO or the PEO·NaI salt-rich complex. This result indicates that all of the PEO present in **3** is incorporated into the complex. In this connection, the size of the anion is known to influence the stoichiometry of PEO complex formation.[12,21] For example, larger anions such as $(C_6H_5)_4B^-$ necessitate more polymer repeat units to solvate one formula weight of salt.[21]

Similar behavior is seen for **1**; no low- or high-melting peaks characteristic of PEO·NaI 3:1 are present, but new endotherms indicate the presence of a different polymer electrolyte: 370 K (broad, weak), 409 K (weak), and 424 K (strong). For compound **4**, a weak glass transition and a single endotherm are present at 253 and 333 K, respectively, with no other features present up to 480 K. Upon cooling and reheating, the glass transition is much stronger and the area under the peak at 333 K is reduced, indicating incomplete crystallization.

X-ray diffraction patterns of PEO-NaI 4:1, **3**, and **4** indicate that these polymer-salt compounds are highly crystalline and distinct from one another. Also no crystallization NaI is present in these cases. DSC, X-ray diffraction, and the colors of these iodine-rich compounds indicate that the complexes of nominal composition PEO_4NaI, PEO_4NaI_2 (**3**), and PEO_4NaI_3 (**4**) are significantly different from each other.

Resonance Raman Spectroscopic Characterization of Polyiodide Species. The formation of polyiodide anions may be thought of as a Lewis acid–base interaction in which I_2 acts as a Lewis acid

(12) Stainer, M.; Hardy, L. C.; Whitmore, D. H.; Shriver, D. F. *J. Electrochem. Soc.* **1984**, *131*, 784–790.
(13) Papke, B. L.; Ratner, M. A.; Shriver, D. F. *J. Electrochem. Soc.* **1982**, *129*, 1434–1438.
(14) Popov, A. I. In *MTP International Review of Science. Inorganic Chemistry*; Gutmann, V., Ed.; University Park Press: Baltimore, MD, 1972; Series 1, Vol. 3, Chapter 2.
(15) Tebbe, K.-F. In *Homoatomic Rings, Chains and Macromolecules of Main-Group Elements*"; Rheingold, A. L., Ed.; Elsevier: New York, 1977; pp 551–606 and references therein.
(16) McLean, R. L.; Bleecher, J. In *Power Sources for Biomedical Implantable Applications and Ambient Temperature Lithium Batteries*; Owens, B. B., Margalit, N., Eds.; The Electrochemical Society, Inc.: Pennington, NJ, 1980; pp 207–219.
(17) Wright, P. V. *Br. Polym. J.* **1975**, *7*, 319–327.
(18) Wright, P. V.; Lee, C. C. *Polymer*, **1982**, *23*, 681–689.
(19) Chiang, C. K.; Davies, G. T.; Harding, C. A.; Aarons, J. *Solid State Ionics* **1983**, *9* and *10*, 1121–1124.
(20) Minier, M.; Berthier, C.; Gorecki, W. *Solid State Ionics* **1983**, *9* and *10*, 1125–1128.
(21) Shriver, D. F.; Papke, B. L.; Ratner, M. A.; Dupon, R.; Wong, T.; Brodwin, M. *Solid State Ionics* **1981**, *5*, 83–88.

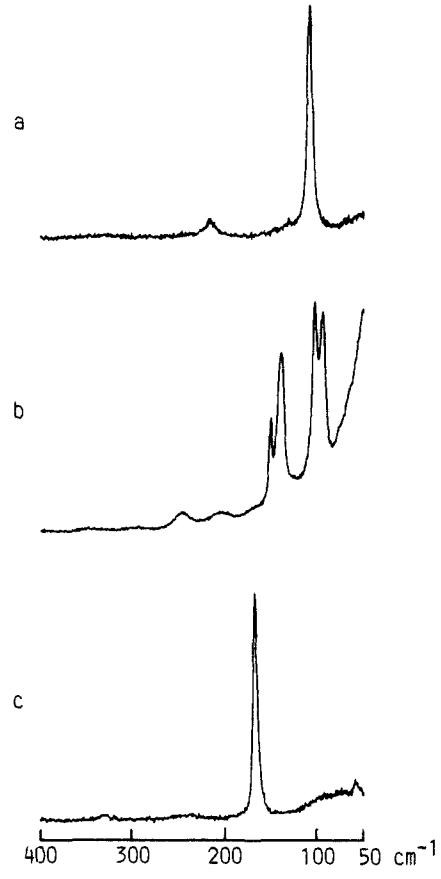

Figure 1. Resonance Raman spectra of model polyiodide compounds: (a) $[Et_4N][I_3]$, (b) CsI_3, (c) $(phenacetin)_4{\cdot}H_2I_4{\cdot}2H_2O$. ($\nu_0$ = 488.0 nm; resolution, 1 cm^{-1}.)

toward the Lewis bases I^- or I_3^-.[15,22] Electron density from the anion is donated to I_2 antibonding orbitals and thus lowers the stretching frequency from 215 cm^{-1} which is observed for I_2 in the gas phase. Resonance Raman spectroscopy is a useful tool for characterizing polyiodide ions.[22] With the large Et_4N^+ counterion, I_3^- is centrosymmetric[23] and gives a simple resonance enhanced Raman band at 111 cm^{-1} (Figure 1a) which is assigned to the totally symmetric I_3^- stretching mode.[24] Under resonance conditions, a series of overtones is observed, at multiples of the fundamental frequency, X-ray structure data for CsI_3 reveal an asymmetric I_3^- moiety,[25] and this lower symmetry is evident in the complex Raman spectrum (Figure 1b) which contains two main stretching frequencies centered at 99 and 145 cm^{-1}.

Raman spectroscopic data for the PEO–sodium polyiodide complexes are summarized in Table I and spectra are shown in Figure 2. For compounds **1** and **3**, simple spectra are observed which are similar to that shown in Figure 1a. The apparent lack of distortion of I_3^- by the complex cation indicates that I_3^- ions are shielded from the small Na^+ cations by coordination of the cations by the polymer. The assignment of I_3^- to the polyiodide formed in **1** and **3** is supported by UV–vis spectroscopy as shown below; therefore, the combination of Raman, UV–vis, and stoichiometry data indicates that I_3^- and I^- coexist in **1** and **3**.

The ratio of I to Na^+ in **2**, **4**, and **5** is never greater than 3:1, so simple I_3^- Raman spectra such as seen for **1** and **3** might be expected. Surprisingly, the spectra for **2** and **5** are more complex and for **4** a shift occurs (Figure 2). All of these spectra contain a band around 171 cm^{-1} which indicates the presence of a polyiodide larger than I_3^-. These observations demonstrate that the concentration of iodine in the polymer electrolyte, as well as the

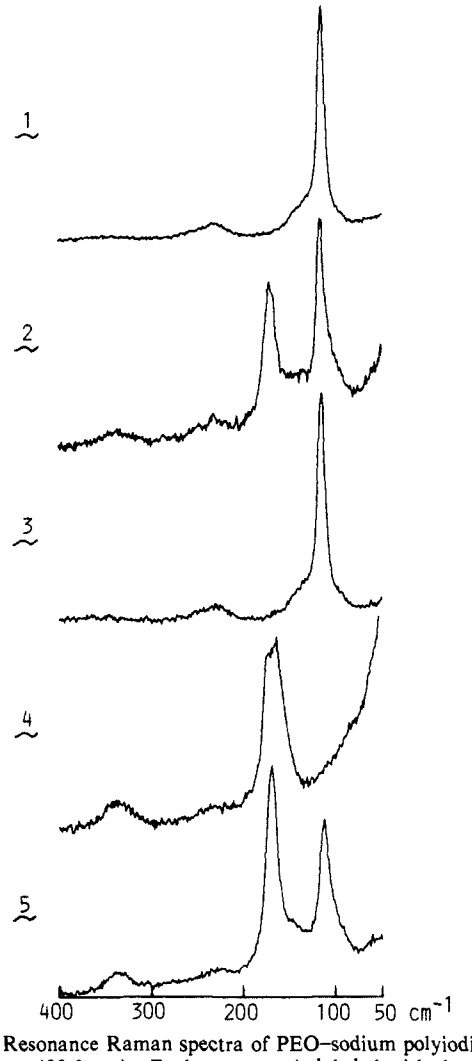

Figure 2. Resonance Raman spectra of PEO–sodium polyiodide compounds (ν_0 = 488.0 nm). Each spectrum is labeled with the material number: **1**, $(PEO)_3NaI_{1.5}$; **2**, $(PEO)_3NaI_2$; **3**, $(PEO)NaI_2$; **4**, $(PEO)_4NaI_3$; **5**, $(PEO)_8NaI_3$.

Scheme I

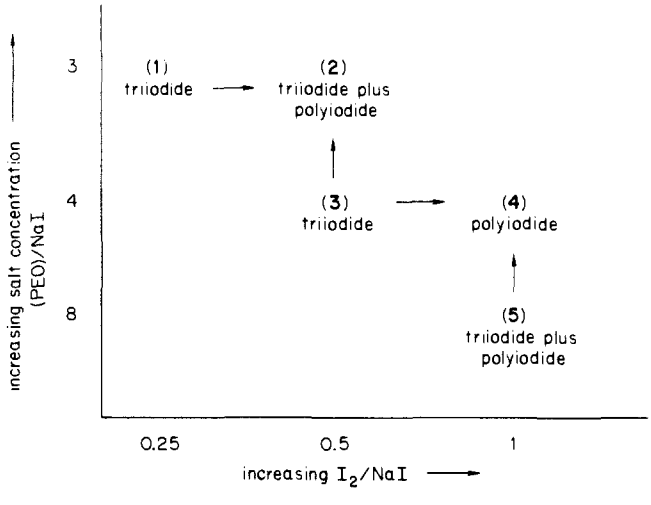

I to Na^+ ratio, influences the formation of polyiodide species. As depicted in Scheme I, the concentration of iodine in the polymer electrolyte may be increased, either by increasing the amount of added I_2 (**1** to **2** and **3** to **4**) or by increasing the salt concentration (**3** to **2** and **5** to **4**). Arrows in the scheme indicate increasing concentration of iodine atoms in the electrolytes. Correlation of these concentration changes to the changes in the Raman spectra of Figure 2 indicates that increasing the iodine concentration in the electrolytes causes conversion of one polyiodide species, pre-

(22) Marks, T. J. *Ann. N.Y. Acad. Sci.* **1978**, *313*, 594–616.
(23) Migchelsen, T.; Vos, A. *Acta Crystallogr.* **1967**, *23*, 796–804.
(24) Gabes, W.; Gerding, H. *J. Mol. Struct.* **1972**, *14*, 267–279.
(25) Runsink, J.; Swen-Walstra, S.; Migchelsen, T. *Acta Crystallogr.* **1972**, *B28*, 1331–1335.

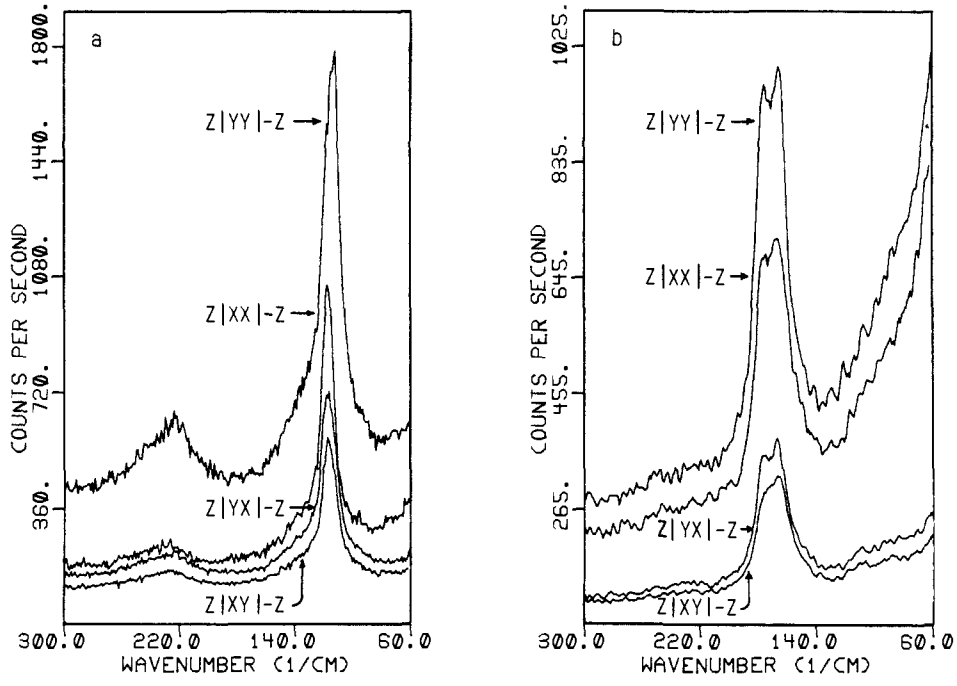

Figure 3. Polarized resonance Raman spectra of oriented fibers (ν_0 = 488.0 nm): (a) **3**, (b) I_2 doped **3**. The fiber axis is in the *Y* direction and the Porto polarization symbols[29a] give the polarization of the incident and sample scattered radiation (in the $+Z$ and $-Z$ propagation directions, respectively).

sumably I_3^- (ca. 111-cm^{-1} peak), to a higher polyiodide species (ca. 171-cm^{-1} peak).

Raman studies of various polyiodide compounds of known structure, in which I_2 is weakly coordinated to I^- or I_3^-, typically show stretching frequencies in the vicinity of 160–187 cm^{-1} for the I_2 moiety in the polyiodide.[22,26] More specifically, when two I_2 moieties are coordinated to one I^- in either a linear or V-shaped fashion, the stretching frequency is centered at ca. 160 cm^{-1}. For I_2 coordinated to I_3^- ions, stretching frequencies of about 170–187 cm^{-1} are typically observed for the perturbed I_2 and peaks are also observed in the 110–120-cm^{-1} range for the I_3^- moieties. The structure of (phenacetin)$_4$·H_2I_4·2H_2O has recently been shown to contain discrete, linear I_4^{2-} ions, $I^-\cdots I—I\cdots I^-$.[27] The Raman spectrum of this compound (Figure 1c) shows only one main stretching frequency at 168 cm^{-1} which is attributed to the I_4^{2-} ion. The single polyiodide stretching frequency in the Raman spectrum of (phenacetin)$_4$·H_2I_4·2H_2O is similar to one in the spectrum for **4**. We take this similarity as an indication of a linear polyiodide array in the polymeric material. An infinite polyiodide chain $(I^-\cdots I—I\cdots)_n$ has been characterized by single-crystal X-ray diffraction[28] in the compound $[Cd(NH_3)_4(I\cdot I_2)_2]$, and this material has very similar iodide–iodine and iodine–iodine bonding distances as observed for $(I^-\cdots I—I\cdots I^-)$ in (phenacetin)$_4$·H_2I_4·2H_2O.[27] Thus it remains that a similar polyiodide chain may occur in **4**. The splitting of the 171-cm^{-1} band that appears in the Raman spectrum for **4** is not readily explained but it may be due to slightly different environments for I_2 adducts or the presence of of a mixture of polyiodides.

The Raman spectra for **2**, **4**, and **5** cannot be explained in terms of a simple mass action equilibrium among I^-, I_3^-, and I_5^-. If these were the only ions present, a large excess of I^- would have to be present to maintain charge balance. For instance, if **2** contains only I^- and I_5^- ions, then the gross composition would require three iodide ions for each I_5^- ion. Alternatively, if **2** contains I_5^-, I_3^-, and I^-, then a ratio of 1:1:4, respectively, would be needed to maintain charge balance. Similarly, an I_5^- species should be present in **3**, but the Raman data show that no I_5^- is present. This analysis suggests that formation of a polyiodide chain as described above is more likely to occur in these PEO–sodium polyiodide compounds.

Table II. Conductivity Values for Polyiodide Compounds at Room Temperature

compound	conductivity (s/cm)	ref
molten polyiodide salts	10^{-2}	42
P2VP·2I_2	10^{-4}	35
$(PEO)_4NaI_3$ (**4**)	2×10^{-5}	this work
$(PEO)_8NaI_3$ (**5**)	1×10^{-5}	this work
$[(CH_3)_4N][I_5]$	5×10^{-8}	32
$[(CH_3)_4N][I_3]$	8×10^{-9}	32

Raman polarization studies[29] on oriented fibers of **3** (Figure 3a) indicate that the C_∞ axes of the I_3^- ions are preferentially oriented in the same direction as the fiber axis. By analyzing the data in Figure 3a according to standard statistical methods,[29b] one obtains $\langle\cos^2\theta\rangle = 0.38$ where $\cos\theta$ is the direction cosine between the C_∞ axis of I_3^- and the fiber axis. By exposing oriented fibers of **3** to I_2 vapor and then to vacuum (2 h, 0.01 torr) the Raman spectra in Figure 3b were obtained and are strikingly similar that seen in Figure 2 for **4**, indicating a probable composition very similar to that of **4**. Polarization studies (Figure 3b) again give $\langle\cos^2\theta\rangle = 0.38$, indicating that the alignment of the C_∞ axis of the I_2 adduct with the fiber axis is of the same degree as for the I_3^- ions in **3**. These studies indicate alignment of the polyiodide was parallel to the net orientation of the polymer chains.

The appearance and electronic spectra vary with composition of the polyiodide-containing polymers so we felt that it was advisable to determine whether the single Raman feature in **4** arises from strong selective resonance enhancement of the Raman scattering of a higher polyiodide, which might obscure a weaker I_3^- scatterer. This possibility appears unlikely because we observed no drastic changes in the spectra of **2** and **5** when the exciting line was changed from 647.1 to 457.9 nm. Also resonance Raman and electronic absorption studies have shown that two main Raman bands are easily detected for polyiodide compounds which have electronic transitions.[26,30,31] similar in nature to those seen for **4**.

(26) Teitelbaum, R. C.; Ruby, S. L.; Marks, T. J. *J. Am. Chem. Soc.* **1980**, *102*, 3322–3328.
(27) Herbstein, F. H.; Kapon, M.; Schwotzer, W. *Helv. Chim. Acta* **1983**, *66*, 35–43.
(28) Tebbe, K.-F.; Plewa, M. *Z. Anorg. Allg. Chem.* **1982**, *489*, 111–125.
(29) (a) Shepherd, I. W. *Adv. Infrared* Raman *Spectrosc.* **1977**, *3*, 127–166 and references therein. (b) Priestly, E. B.; Persham, P. S. *Mol. Cryst. Liq. Cryst.* **1973**, *23*, 369–373.
(30) Robin, M. *J. Chem. Phys.* **1964**, *40*, 3369–3377.
(31) Mizuno, M.; Tanaka, J.; Harada, I. *J. Phys. Chem.* **1981**, *85*, 1789–1794.

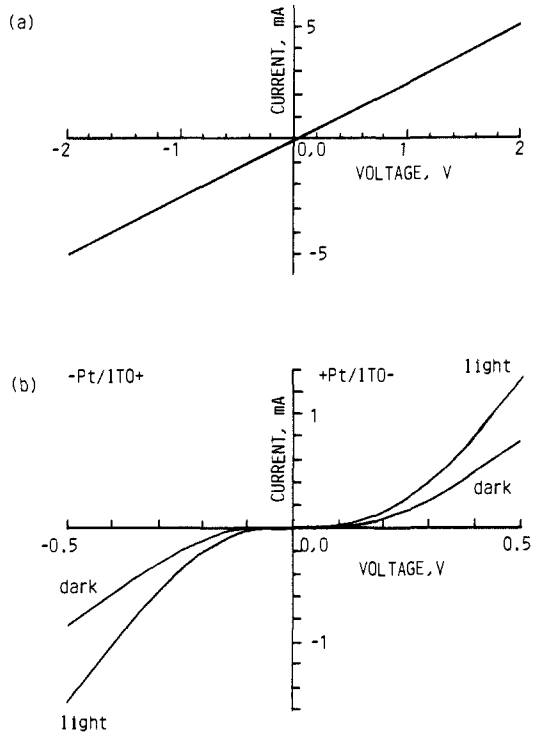

Figure 4. Current–voltage response for $(PEO)_4NaI_3$ (**4**): (a) with symmetric Pt electrodes, (b) one Pt and one ITO electrode, comparison of the response in the dark vs. under illumination.

Electrical and Photoelectrical Properties. Electrical conductivity of polyiodide salts with anions such as I_3^-, I_5^-, and I_7^- has been known for some time,[32,33] and the use of polyiodides as cathode materials in batteries has been proposed.[34] Conductivity values for typical polyiodide conductors and P2VP–I_2[35] are listed in Table II.

The conductivity of quaternary ammonium polyiodide salts has been shown to increase with increasing nuclearity of the polyiodide anion.[32,33] The suggestion was made that the conductivity increased as the distance between polyhalide ions decreased to less than van der Waals radii.[32,33] Subsequent calculations of the band gap energy for $[(CH_3)_4N][I_5]$ substantiated the hypothesis that the iodine framework in the polyiodide salts is important in its effect on the conductivity.[36,37]

Variable-temperature conductivity measurements on $(PEO)_4NaI_3$ (**4**) sandwiched between Pt electrodes indicate an activation energy for charge transport of about 0.7–0.8 eV. The room temperature conductivity is 2×10^{-5} S/cm, or about 2 to 3 orders of magnitude higher than the best conductivities reported among the crystalline polyiodide conductors. Results for different samples from different preparations were fairly reproducible. Upon heating to the melting transition, cooling, and remeasuring the conductivity, values were slightly higher; this behavior may be due to changes in the crystallinity of the compound as indicated by DSC, or perhaps better contact of the polymer to the electrodes. The conductivity of $(PEO)_4NaI_2$ (**3**) was to low to be measured on our vector impedance meter at room temperature, but it was found to be approximately 5×10^{-9} S/cm at 45 °C. (This value for the resistance is only approximate because electrode–electrolyte contact was not optimized owing to the rigid nature of this polymer.) The dramatic increase in conductivity from **3** to **4** correlates with the Raman spectroscopic data presented in the previous section. In the poor conductor, **3**, I_3^- is the predominant polyiodide, whereas the good conductor **4** appears to contain a higher polyiodide.

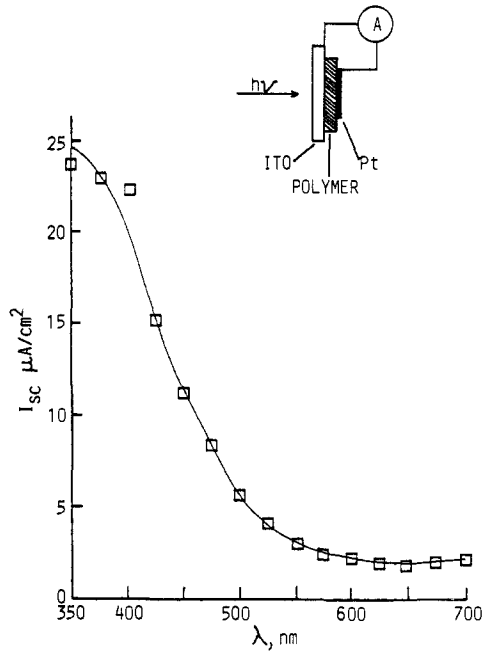

Figure 5. Short-circuit photocurrent (I_{sc}) vs. wavelength for $(PEO)_4NaI_3$ (**4**) and the photovoltaic cell configuration.

In order to properly interpret electrical response data from semiconducting materials, knowledge of the nature of the contact junctions is important.[38a] Current–voltage response and the alternating current complex impedance method[39] were used to characterize the contact behavior of **4** with Pt electrodes. In a set of dc measurements a linear current–voltage response was observed (Figure 4a); this indicates ohmic behavior for **4** between Pt electrodes. Similarly, ac measurements showed that the current and voltage are in phase from ca. 50 kHz to 5 Hz, and the resistances calculated from the ac and dc measurements agree. This electrical response implicates electrons or holes rather than ions as the dominant charge carriers in **4**. Thermoelectric power[40,41a] measurements described in the Experimental Section implicate holes as the majority carriers in **4**.

The conductivities of molten eutectics of iodide salts in iodine have been found to be high,[42] on the order of 10^{-2} S/cm. This electrical conductivity is attributed to both ionic and electronic charge transport, but the latter predominates. The increased conductivity for molten polyiodides over their crystalline counterparts suggests that the conductivity is enhanced by either liquid-like motion or disorder in the polyiodides. Thus liquid-like motion might be required to bring polyiodide chains into close proximity for charge transport. To distinguish a liquid-like motion mechanism from other mechanisms, the conductivity of **4** was measured from −35 °C, through T_g at −20 °C up to room temperature. No break or change in the slope is seen at or near T_g, so a mechanism in which electron hopping is promoted by polyiodide collisions probably does not contribute significantly to the electronic conduction mechanism in **4**.

(32) Kusabayashi, S.; Mikawa, H.; Kawai, S. *Uchida*, M.; Kiriyama, R. *Bull. Chem. Soc. Jpn.* **1964**, *37*, 811–817.
(33) Kusabayashi, S.; Mikawa, H. *Bull. Chem. Soc. Jpn.* **1965**, *38*, 1410–1411.
(34) Owens, B. B.; Oxley, J. E.; Sammells, A. F. In *Solid Electrolytes*; Geller, S.; Ed.; Springer-Verlag: Berlin, 1977; pp 67–104.
(35) Mainthia, S. B.; Kronick, P. L.; Labes, M. M. *J. Chem. Phys.* **1964**, *41*, 2206–2207.
(36) Kusabayashi, S.; Milawa, H. *Bull. Chem. Soc. Jpn.* **1966**, *39*, 736–741.
(37) Kusabayashi, S.; Mikawa, H.; Konda, M.; Hayashi, M. *Bull. Chem. Soc. Jpn.* **1966**, *39*, 1383–1387.
(38) Sze, S. M. *Phyics of Semiconductor Devices*; John Wiley & Sons: New York, 1981; (a) Chapter 5, (b) Chapter 14.
(39) Macdonald, J. R. *J. Chem. Phys.* **1974**, *61*, 3977–3996.
(40) *Semiconductors*; Hannay, N. B., Ed.; Reinhold Publishing Corp.: New York, 1959; pp 40–42.
(41) Mott, N. F.; Davis, E. A. *Electronic Processes in Non-crystalline Materials*; Clarendon Press: Oxford, 1979.; (a) p 235, (b) Chapter 1.
(42) Hayes, T. G.; Owens, B. B.; Phipps, J. B.; Skarstad, P. M.; Untereker, D. F. Abstract 764, p 1126, The Electrochemical Society Extended Abstracts, Vol. 83-1, San Francisco, May 1983, and references therein.

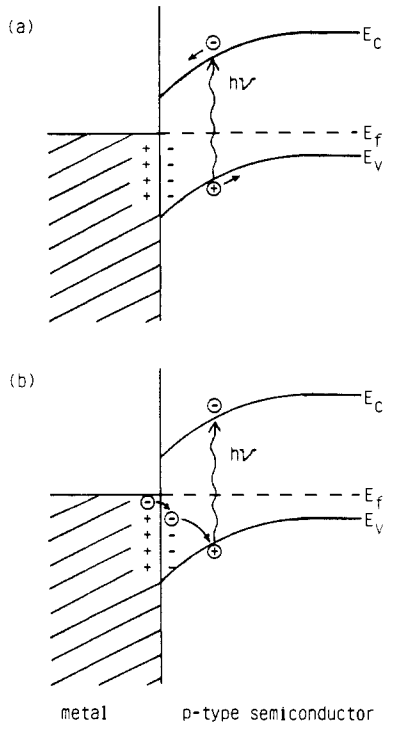

Figure 6. Band diagrams for a Schottky barrier junction with a p-type semiconductor: (a) forward current from photogenerated charge carriers, (b) forward current from recombination.

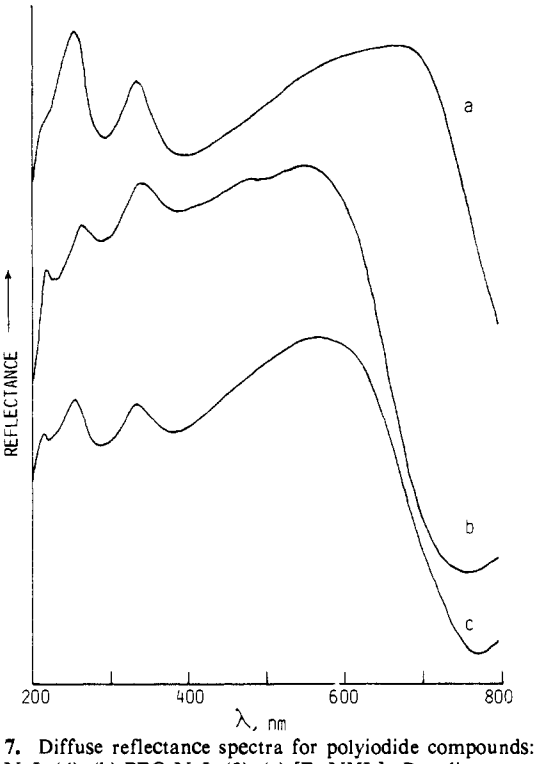

Figure 7. Diffuse reflectance spectra for polyiodide compounds: (a) $(PEO)_4NaI_3$ (**4**); (b) PEO_4NaI_2 (**3**); (c) $[Et_4N][I_3]$. Base lines are offset for comparison.

Organic solids and polymers with photovoltaic properties are of fundamental interest,[43] therefore some of these properties were investigated for **4**. A thick film of the polyiodide containing polymer, **4**, was sandwiched between Pt and indium–tin oxide (ITO) electrodes and illuminated through the ITO as shown in Figure 5. Short-circuit photocurrents (I_{sc}) (Figure 5) and open-circuit voltages (V_{oc}) were easily measured and were found to be on the order of tens of microamps and tens of millivolts under illumination of 0.6 mW/cm^2. These currents and voltages are stable for at least 1 h, and the response time to reach the maximum V_{oc} is less than 0.5 s. When **4** is sandwiched between ITO electrodes, the current–voltage response is nonlinear and shows a diode effect at low voltages. In addition, the complex impedance data reveal part of an arc at high frequencies for bulk response, but at lower frequencies (ca. 50 kHz to 5 Hz) a spur occurs, which is attributed to electronic charge-transfer resistance. Apparently, the ITO electrodes are partially blocking toward the flow of electrons across the electrode–electrolyte interface.

The field which gives rise to the photovoltaic effect is caused by the barrier junction formed at the interface of the polymer and ITO. Indium–tin oxide is a degenerate *n*-type semiconductor,[44,45] so technically the junction could be termed a heterojunction. However, differences between photovoltaic cells using ITO or metal electrodes normally are not noticeable, so the junction may be considered as a simpler Schottky barrier junction.[38b] Optimization of the photovoltaic properties has not been attempted, but rather an understanding of the chemical and physical phenomena which cause the effect was sought. During illumination of a Schottky barrier, charge separation of photogenerated electrons and holes by the field of the junction normally occurs as shown in Figure 6a, with the current mainly due to the electrons. However, if electron mobility[41b] is low or if photogenerated electrons are trapped by states in the gap, excess holes generated by light in the depletion region may recombine with the electrons which form the space-charge region, thus causing an influx of electrons from the metal. As shown in Figure 6b, this process produces a recombination current in the opposite direction from normal Schottky barrier behavior. For the cell configuration shown in Figure 5, and for many practical solar cells,[38b] the observed polarity indicates that recombination predominates (electrons flowing from the ITO to the photoinduced holes in the polyiodide). In addition to the photovoltaic behavior, Figure 4b compares the dark vs. illuminated current–voltage response. The increased currents at higher voltages, under illumination, indicate that **4** is photoconductive.

The photoresponse of Pt/P2VP–I_2/SnO_2 has been reported recently[46] and shows the same direction for the photocurrent and a similar I_{sc} vs. λ response as for **4**. These similarities suggest that the photovoltaic process for both systems can be attributed to the iodine species. However, the photoconductive response for the two polymer systems is different. For dark vs. light currents, **4** shows greater light currents at higher applied voltages (Figure 6b), but for the P2VP–I_2 system light and dark currents are similar at higher fields (>0.4 V). The differences in the photoconductive response of the two systems are not readily explained and may be due to differences in the polyiodides or suppression of the photoconductivity mechanism in P2VP–I_2 at higher fields. The efficiency of the P2VP–I_2 photovoltaic cell[46] is 0.05%, and by comparison the efficiency of the cell made with **4** appears to be somewhat less than 0.05%.

UV–vis spectroscopy of the PEO–polyiodide materials was investigated to help identify the polyiodide species and perhaps learn more about the electrical processes. Because of the high optical density of some samples, diffuse reflectance rather than absorption spectra were collected in some cases. The reflectance spectrum of **4** is shown in Figure 7a; in the near-IR region, the normal overtones and combination bands are observed for the methylene groups. At higher energies the onset of broad absorption occurs around 850 nm and continues through the UV region. Comparison of the optical gap, approximately 1.5 eV, with the activation energy for conductivity, ca. 0.7–0.8 eV, yields the relationship $^1/_2 E_{op} = E_a$, which often is observed for amorphous

(43) Merrit, V. Y. In *Electrical Properties of Polymers*; Seanor, D. A., Ed.; Academic Press: New York, 1982; Chapter 4.
(44) Manifacier, J. C.; Fillard, J. P.; Bind, J. M. *Thin Solid Films* **1981**, *77*, 67–80.
(45) Fehrenbruch, A. L.; Bube, R. H. *Fundamentals of Solar Cells*; Academic Press: New York, 1983; Chapter 11.
(46) Vander Donckt, E.; Noirhomme, B.; Kanicki, J.; Deltour, R.; Gusman, G. *J. Appl. Polymn. Sci.* **1982**, *27*, 1–9.

Table III. Electronic Absorption and Reflectance Data for Various Polyiodide Compounds[a]

compound	absorption		reflectance
	I^-	I_3^-	I_3^-
I^-, I_3^- (solution)	193, 220[b]	292, 363, 531[c]	
$(PEO)_4NaI$/dilute in I_3^-	193, 225	290, 360	290, 360
3, translucent	193, 220	305, 370	268, 340, 438
3, opaque			265, 338, 480, 550
4, opaque			255, 333, 670
$[Et_4N][I_3]$, opaque			255, 333, 570

[a] Wavelength in nm. [b] From ref 31. [c] From ref 49.

and liquid semiconductors.[47] The conduction mechanism in **4** may be similar to that seen for an amorphous material where energy states are localized[41b] and conduction occurs by a hopping mechanism.

Comparison of the reflectance spectra of the triiodide-containing polymer **3** and $[Et_4N][I_3]$ (Figure 4b,c) shows that these two compounds have very similar electronic transitions, and the peaks in the UV region are very similar to those observed for **4** (Figure 7a). The band maximum in the visible region, however,, is shifted ca. 110 nm to lower energy for **4** in comparison to the triiodide-containing species. The UV peaks in Figure 7 appear to corresponds to the energy where the maximum is approached in the I_{sc} vs. λ spectrum. Correspondence between reflectance and transmittance spectroscopy was investigated to attempt a tentative assignment to the UV transitions because the I_{sc} response spectrum should resemble the absorption spectrum if excited state species dissociate to give current carriers when illumination occurs through the barrier junction.[43]

Good correspondence between reflectance and absorbance spectroscopy normally occurs if the chromopheric sites are dilute. However, when concentrated samples are used, red shifts occur in the reflectance spectra owing to different wavelength dependencies of scattering parameters and absorption coefficients.[48] Table III summarizes the absorption and reflectance data for various thin and thick sample films as well as I_3^- in solution and $[Et_4N][I_3]$ solid. Band maxima for I_3^- occur at the same wavelength for absorption and reflectance techniques if I_3^- is very dilute in PEO·NaI 4:1 (Figure 8a); in addition, characteristic UV absorptions are seen for I^-. For example, band maxima values for the dilute species agree with values reported for I^- in aqueous solution (193 and 220 nm)[31] and I_3^- in acetonitrile (293 and 363 nm).[49] For a translucent film of the concentrated compound **6**, the absorption spectrum is red-shifted slightly, about 15 nm, but the reflectance spectrum of the same film appears quite different (Figure 8b,c). In the reflectance spectrum (Figure 8c) the main bands for I_3^- are red shifted and a new band at 268 nm appears, as is also seen for $[Et_4N][I_3]$ and is not attributed to absorptions for I^- which appear at higher energies. Also notable is a large change in the intensity of a weak I_3^- absorption as observed in the reflectance spectra of translucent vs. opaque films of **3** (Figure 8c,d).

Detailed assignments for the electronic transitions of I_3^- have recently been established through analysis of the electronic and magnetic circular dichroism spectra.[49] Because of the similar UV absorptions in triodide ion and **4**, the possibility exists that the UV electronic transitions in **4** are very similar to those assigned to I_3^- and these transitions may give rise to the excited-state species which dissociate to give current carriers in the photovoltaic process.

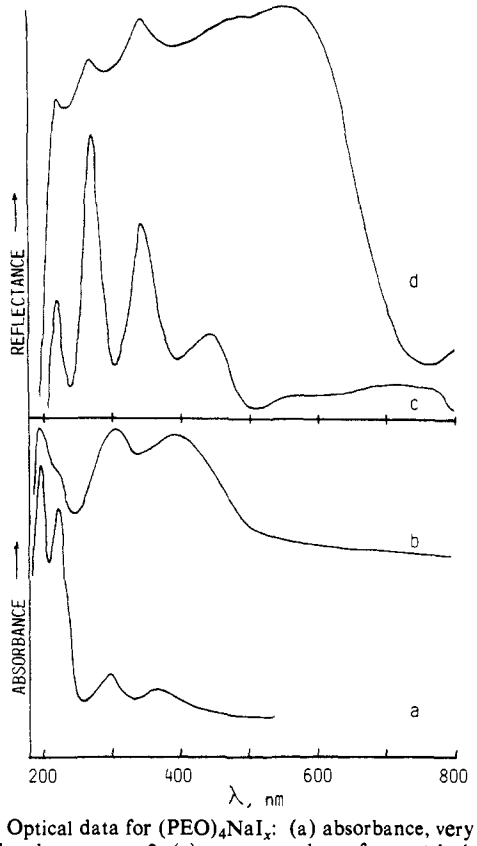

Figure 8. Optical data for $(PEO)_4NaI_x$: (a) absorbance, very dilute in I_3^-; (b) absorbance, $x = 2$; (c) same sample as for part b, but in the reflectance mode; (d) reflectance, $x = 2$, thick, opaque sample. Base lines are offset for comparison.

Conclusions

Electrical properties of solid polymer–salt complexes may be tailored to include electronic as well as ionic conductivity by proper choice of anions and by control of the salt concentration. In the polyiodide systems studied here conductivity appears to coincide with the formation of an extended polyiodide. The conductivity in the flexible, semicrystalline material $(PEO)_4NaI_3$ (**4**) is about three orders of magnitude greater than in solid, simple quaternary ammonium polyiodide salts, three orders of magnitude less than in molten polyiodide salts, and about a factor of five less than in the P2VP–I_2 system.

The photovoltaic behavior observed for **4** is attributed to a barrier contact of the junction with the tin-doped indium oxide current collector. Similarities between the photovoltaic properties of P2VP–I_2 and **4** are evident and probably occur because of similar mechanisms for charge generation and separation at the barrier junction. But differences found in the photoconductive behavior of the two polymers are likely to be due to differences in the conduction mechanisms in the bulk materials and the effect of an applied field on these mechanisms.

Although only polyiodide ion conductors are reported here, polyethylene oxide and other polar polymers should be suitable hosts for a variety of salts which permit electron or hole transport. One of the attractive features of these polymers-based salt complexes is the freedom to vary the concentrations and nature of the charge carriers.

Acknowledgment. This research was supported by the Office of Naval Research and facilities were provided by the NSF Materials Research Laboratory Program through the Northwestern University Materials Research Center. We appreciate helpful conversations with Joseph Lomax and Professor Mark Ratner.

(47) Fritzsche, H. In *Amorphours and Liquid Semiconductors*; Tauc, J., Ed.; Plenum Press: New York, 1974.
(48) Kortum, G. *Reflectance Spectroscopy*; Springer-Verlag: New York, 1969; Chapter 5.
(49) Isci, H.; Mason, R. W. *Inorg. Chem.* **1985**, *24*, 271–274.